J Mater Sci (2008) 43:197–202
DOI 10.1007/s10853-007-2133-5

Effects of synthetic conditions on the structure and electrical properties of polyaniline nanofibers

Chang Su · Gengchao Wang · Farong Huang · Xingwei Li

Received: 4 July 2007 / Accepted: 28 August 2007 / Published online: 29 September 2007

Abstract Polyaniline nanofibers were synthesized by interfacial polymerization in the presence of hydrochloric acid ($HClO_4$). The effects of the molar ratio of ammonium persulfate (APS) to aniline (ANI) (represented by [APS]/[ANI] ratio) and $HClO_4$ concentration on the morphology, chain structures, and electrical properties of the polyaniline (PANI) were investigated to understand the formation of nanofibers. The structure and properties of the resulted PANI were characterized with FTIR, UV–Vis, TEM, XRD, and conductivity in detail. The results showed that low [APS]/[ANI] ratio (≤1/4) and high $HClO_4$ concentration (≥1000 mol/m^3) were benefit to the preparation of uniform PANI nanofibers with low content of phenazine-like units and ANI oligomers, and high conductivity.

Introduction

Nanostructured (nanofibers/nanowires/nanotubes) conducting polymers have received great attention due to their unique properties and promising application in nanomaterials and nanodevice. Of all conducting polymers, polyaniline (PANI) is extensively studied owing to its low cost, excellent environmental stability, and unique redox properties. The nanostructured PANI has been applied in chemical sensors, energy conversion and storage, light-emitting display devices, microelectronics, optical storage, and so on [1]. Usually, PANI nanofibers can be prepared by hard-template polymerization [2, 3], soft-template polymerization [4, 5], seeding-guided polymerization [6], electrospinning [7, 8], electrochemical polymerization [9, 10], interfacial polymerization [11–15], rapidly mixed reaction [16], and dilute polymerization [17]. Among these methods, interfacial polymerization is one of the most effective means, which produces high-quality PANI nanofibers in large quantities. Previously correlative work has been expended toward the effect of doping acids, solvents, polymerization temperature, and monomer concentration on the morphology of PANI nanofibers [12, 14] in the interfacial polymerization. However, less attention has been paid to the effects of synthetic conditions on the molecular structure and electrical properties. Since the oxidant and doping acids play an important role in controlling the morphology, structure, and physical properties of PANI, thus it is necessary to study the effects of oxidant content and acid concentration on the structure and electrical properties of PANI during the interfacial polymerization in order to prepare high-quality PANI nanofibers by interfacial polymerization.

In this article, PANI nanofibers were prepared by interfacial polymerization in the presence of $HClO_4$. The influence of [APS]/[ANI] ratio and $HClO_4$ concentration on the morphological structure, chain structure, crystallinity, and electrical properties was investigated.

Experimental

Materials

Aniline (ANI, analytical grade) was purchased from Shanghai Chemical Reagent Co. and distilled under

C. Su · G. Wang (✉) · F. Huang · X. Li
Key Laboratory for Ultrafine Materials of Ministry of Education, School of Materials Science and Engineering, East China University of Science and Technology, Shanghai 200237, P.R. China
e-mail: gengchaow@ecust.edu.cn

vacuum prior to use. Ammonium persulfate (APS, analytical grade) was purchased from Shanghai Lingfeng Chemical Reagent Co. and was purified by recrystallization from ethanol. Chloroform, $HClO_4$, and ammonium hydroxide as analytical grade were used without further purification.

Synthesis of PANI nanofibers

PANI nanofibers doped with $HClO_4$ were synthesized according to the previous described interfacial polymerization procedure [11]. Typical preparation process was as follows: 2.98 g (32 mmol) of ANI were dissolved in 100-mL chloroform and various amounts of APS ([APS]/[ANI] ratio of 1/6, 1/4, 1/2, and 1/1) were dissolved in 100 mL of 1,000 mol/m^3 $HClO_4$ solution. The ANI solution and $HClO_4$ solution were then carefully transferred to a 250-mL beaker. The reaction was carried out at the interface of the two phases at room temperature for 24 h. The resulting black precipitates were filtered and rinsed with deionized water for several times to obtain protonated PANI nanofibers. In order to study the effect of $HClO_4$ concentration, PANI nanofibers were also prepared at [APS]/[ANI] ratio of 1/4 by using the above process and $HClO_4$ concentration varied from 500 to 3,000 mol/m^3. Dedoped nanofibers were obtained by the treatment of $HClO_4$-doped PANI with 10 wt% of ammonia aqueous solution for 24 h.

Instrumentation

Transmission electron microscopy (TEM, JEM-100CXII) was employed to observe the morphology of products. The power samples for TEM were dispersed in ethanol under ultrasonic irradiation, and then coating onto wholly carbon-coated copper girds. Fourier transform infrared spectra (FTIR) were recorded from KBr sample pellets using a Nicolet 5700 spectrometer with a resolution of 2 cm^{-1}. The UV–Vis spectra were recorded on a Shimadzu UV-250 spectrophotometer. X-ray diffraction (XRD) patterns were obtained by a Rigaku D/Max-RB X-ray diffractometer using Cu Kα radiation. The diffraction data were recorded at 2θ angles varying between 3° and 50°. The electrical conductivity of compressed PAIN pellets was measured by a four-probe method with a SX 1934 four-probe instrument.

Results and discussion

Effects of [APS]/[ANI] ratio

The morphology of the resulting PANI polymerized at the different [APS]/[ANI] ratio is shown in Fig. 1. The PANI nanofibers with the diameters from 70 to120 nm are synthesized at low [APS]/[ANI] ratio (≤1/4) (Fig. 1a, b). However, with the increase of [APS]/[ANI] ratio, the fibrillar morphology becomes more and more aggregation (Fig. 1c). Finally, the fibrillar morphology of PANI has almost disappeared when synthesized at [APS]/[ANI] ratio of 1/1 (Fig. 1d).

The formation of PANI nanofibers is probably related to the oxidative chemical polymerization process of ANI and the linear nature of PANI chains in the initial stage of polymerization [15]. For traditional oxidative chemical polymerization, the freshly formed PANI initially exists in a fibrillar form. These fibrillar PANI will likely become the "nucleation" centers for further polymerization of ANI and PANI precipitation, which finally grow into irregularly shaped agglomerates. Thus, the suppression of secondary growth is an effective way for the final PANI nanofibers. In the interfacial polymerization, the polymerization occurs only at the interface of two phases, when these newly formed PANI nanofibers move away from the interface and diffuse into the water phase, the polymerization and self-aggregation are terminated. As a result, secondary growth of nanofibers is suppressed to form PANI nanofibers. At low [APS]/[ANI] ratio, since the concentration of oxidant (APS) is low, the numbers of the initial nanofibers are also less, which effectively suppresses the aggregation of the initially formed PANI nanofibers. At high [APS]/[ANI] ratio, the concentration of the initially fibrous PANI increases, resulting in the PANI nanofibers aggregate quickly together to form irregular shape before entering aqueous phase.

The molecular structure of PANI synthesized at the different [APS]/[ANI] ratio is identified by FTIR and

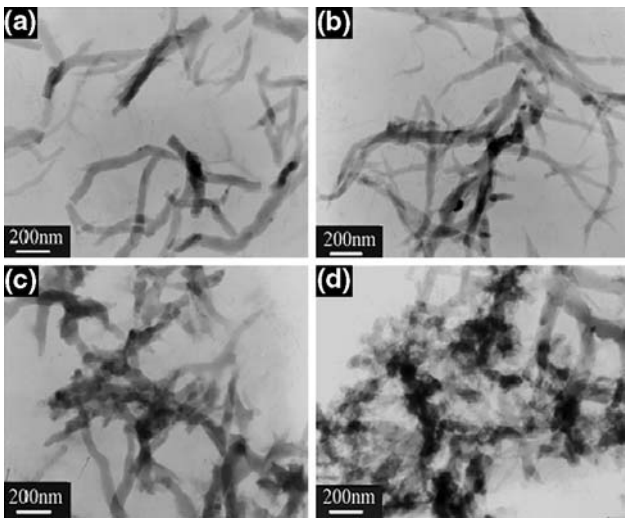

Fig. 1 TEM images of PANI nanofibers made by interfacial polymerization with the different [APS]/[ANI] ratio: (**a**) 1/6, (**b**) 1/4, (**c**) 1/2, and (**d**) 1/1

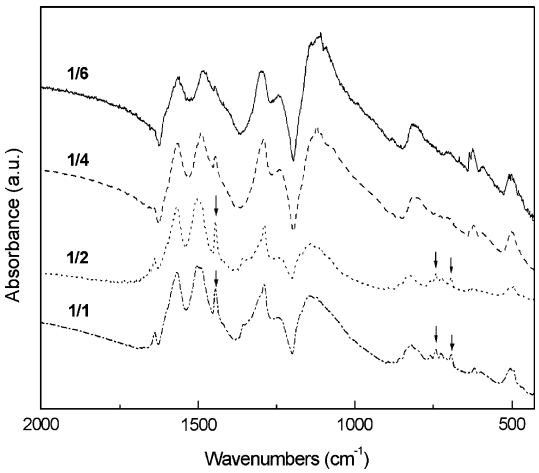

Fig. 2 FTIR spectra of PANI nanofibers made by interfacial polymerization with different [APS]/[ANI] ratio: 1/6 (solid line), 1/4 (dash line), 1/2 (dot line), and 1/1 (dash dot line)

UV–Vis spectra. Figure 2 shows the FTIR spectra of PANI synthesized at different [APS]/[ANI] ratio. The FTIR spectra of all samples exhibit the clear presence of the quinoid ring vibrations (1,565 cm^{-1}) and benzoid ring vibrations (1,490 cm^{-1}) of the emeraldine salt (ES) form [18]. The strong characteristic peak appearing at 1,120–1,140 cm^{-1}, described by MacDiarmid et al. [19] as the "electron-like band", shifts from low wavenumber (1,122 cm^{-1}) to high wavenumber (1,143 cm^{-1}), following with the decreasing peak intensity, with the increase of [APS]/[ANI] ratio, indicating that the degree of delocalization of electrons decreases. Compared with low [APS]/[ANI] ratio, the peaks at about 1,442 cm^{-1}, 742 cm^{-1}, and 692 cm^{-1} are observed at high [APS]/[ANI] ratio (1/2 and 1/1), which are related to the presence of phenazine-like segments [20] and ANI oligomers [21–23].

Figure 3 shows the UV–Vis spectra of dedoped PANI dispersed in water. The obtained PANI at low oxidant content ([APS]/[ANI] ratio ≤ 1/4) exhibit two absorption bands: The band at 330–335 nm corresponds to π–π^* transition, the band around 670–690 nm attributes to n–π^* transition [24]. With the increasing [APS]/[ANI] ratio to 1/2, a new band at about 439 nm appears, which is assigned to the absorption of phenazine-like segments [25], indicating the formation of phenazine-like unites on the PANI chain. In addition, the band of π–π^* transition blueshifts to 296 nm. The hypsochromic shift of the π–π^* transition band is in accord with a decreasing extent of conjugation due to the presence of the phenazine-like unites and the ANI oligomers. As [APS]/[ANI] ratio reaches 1/1, the n–π^* transition band blueshifts to 603 nm, comparing with the decrease of band intensity. This suggests that the extent of conjugation decreases further.

The XRD patterns for the samples are shown in Fig. 4. As shown in Fig. 4, the XRD patterns of all samples exhibit two diffraction peaks at about 19° and 26°, indicating that the nanofibers are partially crystalline as previously reported [25]. With the increasing of [APS]/[ANI] ratio, the intensity of two peaks grows stronger and a new peak at 7° occurs. According to the report [26], PANI oligomers present the multiple peaks with high intensity. Thus, the presence of more oligomers and phenazine-like unites in the product are possibly responsible to the stronger diffraction peaks and the new peak at 7°.

The influence of the [APS]/[ANI] ratio on the conductivity is presented in Table 1. The electrical conductivity of the samples decreases with the increase of the oxidant content. Specially, the conductivity of PANI nanofibers synthesized at low [APS]/[ANI] ratio (1/6–1/4) is one order of magnitude higher than that of PANI nanofibers at high [APS]/[ANI] ratio (1/2–1/1). The low conductivity of

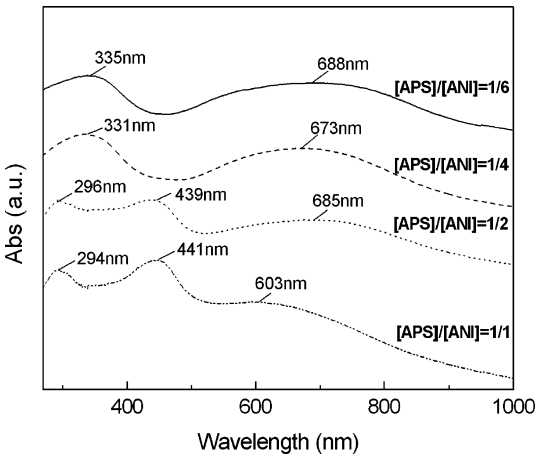

Fig. 3 UV–Vis spectra of dedoped PANI nanofibers made by interfacial polymerization with different [APS]/[ANI] ratio: 1/6 (solid line), 1/4 (dash line), 1/2 (dot line), and 1/1 (dash dot line)

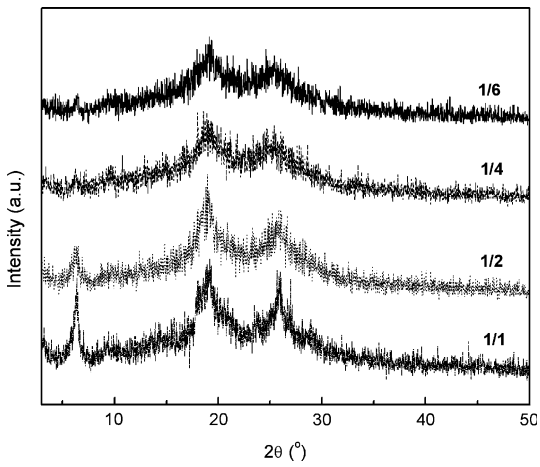

Fig. 4 X-ray diffraction patterns of PANI nanofibers made by interfacial polymerization with different [APS]/[ANI] ratio: 1/6 (solid line), 1/4 (dash line), 1/2 (dot line), and 1/1 (dash dot line)

Table 1 Effects of [APS]/[ANI] molar ratio on the electrical conductivity of PANI made by interfacial polymerization[a]

[APS]/[ANI] molar ratio	1/6	1/4	1/2	1/1
Conductivity (S/cm)	8.6	2.0	0.21	0.16

[a] The reaction conductions: [ANI] = 320 mol/m^3, 1500 mol/m^3, $HClO_4$ = 100 mL, $CHCl_3$ = 100 mL, reaction time = 20 h, at room temperature

PANI synthesized at high [APS]/[ANI] ratio is attributed to the more ANI oligomers and the phenazine-like unites on PANI chain, which decreases the degree of electron delocalization.

Effects of $HClO_4$ concentration

The effect of $HClO_4$ concentration on the PANI morphology is shown in Fig. 5. The morphology of PANI nanofibers in low $HClO_4$ concentration (500 mol/m^3) is indistinct and aggregated (Fig. 5a). With the increase of $HClO_4$ concentration from 1,000 to 3,000 mol/m^3, the fibrillar morphology gradually becomes uniform, which comprises the less aggregate structure (Fig. 5b–d). The diameters of the nanofibers decrease slightly from 120 to 80 nm with the increasing $HClO_4$ concentration.

The aforementioned results indicate that the $HClO_4$ concentration affects the morphology of PANI. At low $HClO_4$ concentration (500 mol/m^3), the hydrophilicity of PANI nanofibers is bad due to low doped extent on PANI chains, which leads to that generated PANI nanofibers stay at the interface for a long time before diffusing into aqueous phase. As a result, the aggregation of newborn

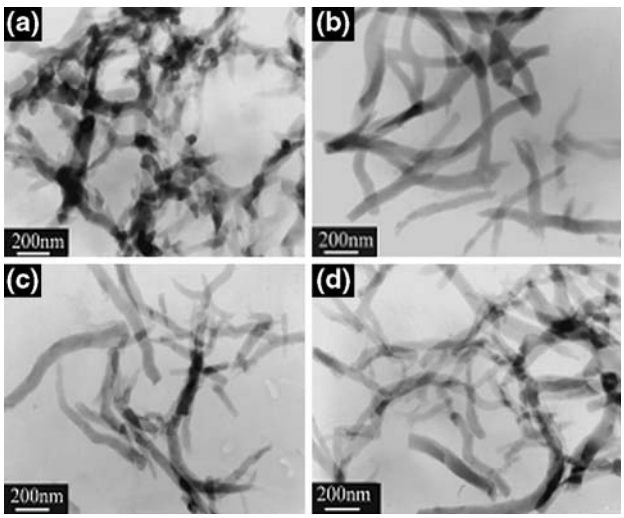

Fig. 5 TEM images of PANI nanofibers made by interfacial polymerization under different $HClO_4$ concentration: (**a**) 500 mol/m^3, (**b**) 1,000 mol/m^3, (**c**) 2,000 mol/m^3, and (**d**) 3,000 mol/m^3

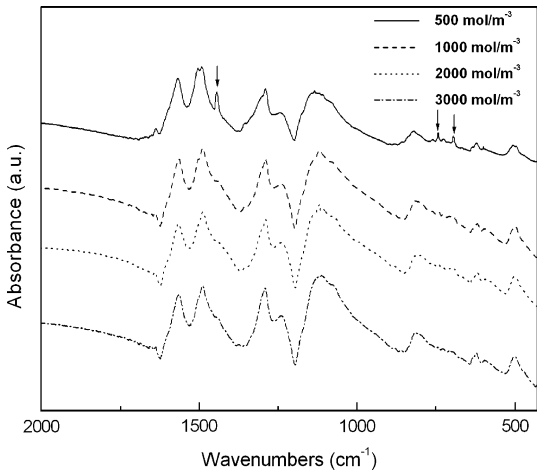

Fig. 6 FTIR spectra of PANI nanofibers made by interfacial polymerization under different $HClO_4$ concentration: 500 mol/m^3 (solid line), 1,000 mol/m^3 (dash line), 2,000 mol/m^3 (dot line), and 3,000 mol/m^3 (dash dot line)

PANI chains on initial fibrillar nucleation sites becomes more serious, which results in indistinct structure. With the increasing of $HClO_4$ concentration, the doped degree and the hydrophilicity of PANI nanofibers increase correspondingly, which leads to the resulted PANI nanofibers diffuse quickly into aqueous phase. Therefore, the overgrowth and aggregation of PANI nanofibers are suppressed.

Figure 6 shows FTIR spectra of the doped PANI synthesized in different $HClO_4$ concentration. Obviously, the "electronic-like absorption" band shifts from 1,133 to 1,112 cm^{-1}, as $HClO_4$ concentration changes from 500 to 3000 mol/m^3. At the same time, the intensity of the peaks becomes stronger with increasing $HClO_4$ concentration. This is possibly because the doped degree of PANI increases with the increasing $HClO_4$ concentration, which results in the high degree of delocalization of electrons along PANI chain. In addition, PANI nanofibers prepared at 500 mol/m^3 $HClO_4$ concentration exhibit three new absorption peaks at about 1,442 cm^{-1}, 742 cm^{-1}, and 692 cm^{-1}, which indicates that the phenazine-like unites and the ANI oligomers are produced at low $HClO_4$ concentration.

The UV–Vis spectra of the dedoped PANI synthesized in different $HClO_4$ concentration are given in Fig. 7. The dedoped PANI obtained in high $HClO_4$ concentration (1,000–3,000 mol/m^3) exhibit two absorption bands at 345 nm and 660–690 nm corresponds to π–π^* transition and n–π^* transition, respectively, which is similar to PANI emeraldine base [24]. The n–π^* transition band blueshifts with the decrease of $HClO_4$ concentration, which indicates that the extent of conjugation of PANI chain decreases. For dedoped PANI polymerized at 500 mol/m^3 $HClO_4$ concentration, there are some changes about absorption bands: the absorption peak of the π–π^* transition blueshifts to

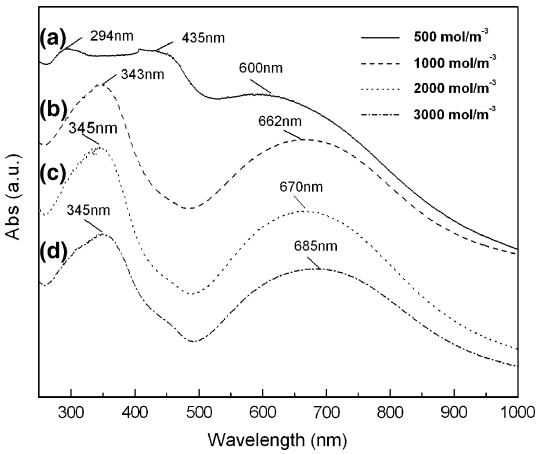

Fig. 7 UV–Vis spectra of dedoped PANI nanofibers made by interfacial polymerization under different $HClO_4$ concentration: 500 mol/m^3 (solid line), 1,000 mol/m^3 (dash line), 2,000 mol/m^3 (dot line), and 3,000 mol/m^3 (dash dot line)

294 nm, a new band appears at 435 nm and the n–π* excitation band blueshifts to 600 nm. In this case, the phenazine-like unites and the ANI oligomers are responsible for the hypsochromic shift of absorption bands and the appearance of the new band.

The X-ray diffraction patterns of the PANI nanofibers are shown in Fig. 8. For PANI synthesized at 500 mol/m^3 $HClO_4$ solution, the three stronger diffraction peaks at ~7°, 19°, and 26° are observed. With the increasing of $HClO_4$ concentration, the peak at ~7.0° disappears and two peaks at ~19° and 26° become weaker. This indicates that the high crystallinity and the appearance of a new peak at 7° contribute to the generation of the phenazine-like unites and ANI oligomers produced at low $HClO_4$ solution.

The effect of the $HClO_4$ concentration on the electrical conductivity of PANI is presented in Table 2. The

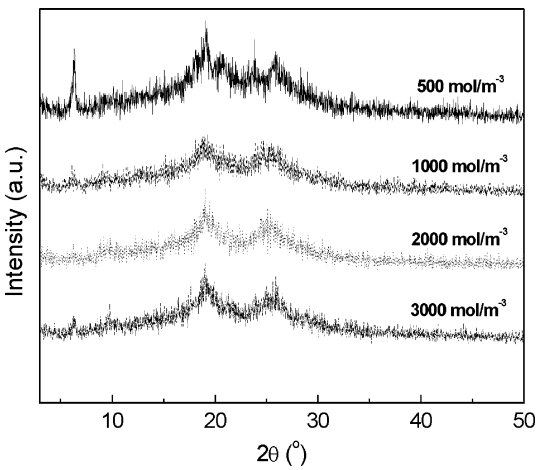

Fig. 8 X-ray diffraction patterns of PANI nanofibers made by interfacial polymerization under different $HClO_4$ concentration: 500 mol/m^3 (solid line), 1,000 mol/m^3 (dash line), 2,000 mol/m^3 (dot line), and 3,000 mol/m^3 (dash dot line)

Table 2 Effects of $HClO_4$ concentration on the electrical conductivity of PANI nanofibers made by interfacial polymerization[a]

$HClO_4$ acidity (mol/m^3)	500	1000	2000	3000
Conductivity (S/cm)	0.16	1.5	2.1	4.3

[a] The reaction conditions: [ANI] = 320 mol/m^3, [APS]/[ANI] = 1/4, $CHCl_3$ = 100 mL, reaction time = 20 h, at room temperature

electrical conductivity of PANI increases with the increasing of $HClO_4$ concentration. Specially, the conductivity increases one order of magnitude as the $HClO_4$ concentration increases from 500 to 1,000 mol/m^3. The doping degree and chain structure of PANI are responsible for the change of electrical conductivities. At low $HClO_4$ concentration (500 mol/m^3), the generated ANI oligomers and the phenazine-like structure in the PANI chains destroyed electron delocalization along with PANI chains, resulting in obvious decrease of the conductivity. With the increasing of $HClO_4$ concentration, the doping degree of PANI increases and ANI oligomers content decreases, which results in higher conductivity.

Conclusions

The effect of [APS]/[ANI] ratio and $HClO_4$ concentration on the morphology, chain structure, and electrical properties were investigated. At low [APS]/[ANI] ratio (≤1/4) and high $HClO_4$ concentration (≥1,000 mol/m^3), the regular PANI nanofibers with the diameters in the range of 70–120 nm and the high conductivity (1–10 S/cm) were obtained. In contrast, at high [APS]/[ANI] ratio and low $HClO_4$ concentration, the morphology of nanofibers became indistinct. The studies of FTIR and UV–Vis spectra indicated that the presence of ANI oligomers and phenazine-like structure in the PANI chain, resulting in the lower conductivity.

Acknowledgements We greatly appreciate the financial supports of the National Natural Science Foundation of China (no: 20236020), and the Key Programs of Ministry of Education of China (no: 106074).

References

1. Huang JX, Kaner RB (2006) Chem Commun (6):367
2. Martin CR, Van Dyke LS, Cai Z, Liang W (1990) J Am Chem Soc 112:8976
3. Martin CR (1994) Science 266:1961
4. Qiu HJ, Wan MX, Matthews B, Dai LM (2001) Macromolecules 34:675
5. Liu J, Wan MX (2001) J Mater Chem 11:404
6. Zhang XY, Goux WJ, Manohar SK (2004) J Am Chem Soc 126:4502

7. MacDiarmid AG, Jones WE, Norris ID, Gao J, Johnson AT, Pinto NJ, Hone J, Han B, Ko FK, Okuzaki H, Llaguno M (2001) Synth Met 119:27
8. Pinto NJ, Johnson AT, MacDiarmid AG, Mueller CH, Theofylaktos N, Robinson DC, Miranda FA (2003) Appl Phys Lett 83:4244
9. Choi SJ, Park SM (2002) J Electrochem Soc 149:26
10. Liang L, Liu J, Windisch CF, Exarhos GJ, Lin YH (2002) Angew Chem Int Ed 41:3665
11. Huang JX, Virji S, Weiller BH, Kaner RB (2003) J Am Chem Soc 125:314
12. Huang JX, Virji S, Weiller BH, Kaner RB (2004) Chem Eur J 10:1314
13. Hopkins AR, Sawall DD, Viaalhermosa RM, Lipeles RA (2004) Thin Solid Films 469–470:304
14. Zhang XY, Chan-Yu-King R, Jose A, Manohar SK (2004) Synth Met 145:23
15. Huang JX, Kaner RB (2004) Angew Chem Int Ed 116:5941
16. Huang JX, Kaner RB (2004) Angew Chem Int Ed 43:5817
17. Chiou NR, Epstein AJ (2005) Adv Mater 17:1679
18. Furukawa Y, Ueda F, Hyodo Y, Harada I, Nakajima T, Kawagoe T (1988) Macromolecules 21:1297
19. Kaplan S, Conwell EM, Richter AF, MacDiamid AG (1985) J Am Chem Soc 161:419
20. Miroslava T, Ivana S, Elena NK, Jaroslav S, Petr H, Gordana CM (2006) J Phys Chem B 110:9461
21. Boyer MI, Quillard S, Rebourt E, Louarn G, Buisson JP, Monkman A, Lefrant S (1998) J Phys Chem B 102:7382
22. Quillard S, Boyer MI, Cochet M, Buisson JP, Lefrant S (1999) Synth Met 101:768
23. Konyushenko EN, Stejskal J, Šeděnková I, Trchová M, Sapurina I, Cieslar M, Prokěs J (2006) Polym Int 55:31
24. Phillips SD, Yu G, Heeger AJ (1989) J Phys Rev B 39:10702
25. Salma B, Rudolf H (2007) Electrochimica Acta 52:5346
26. Laska J, Widlarz J (2005) Polymer 46:1485